Proceedings of the 21st ICSMGE, Vienna, Austria, 14 – 19 June 2026. Pistrol, Adam & Schweiger (eds.)
Published by: ÖGG, Austrian Society for Geomechanics, Salzburg, Austria, ISBN 978-3-9503898-4-5
https://doi.org/10.53243/ICSMGE2026-450

Optimization of advanced constitutive model parameters for deep excavation analysis using multi-objective particle swarm optimization

Kevin Raharja, **Fu-Hsuan Yeh**, I-Tung Yang, Fu-Chen Teng
Department of Civil and Construction Engineering, National Taiwan University of Science and Technology, Taiwan (R.O.C.), *fhyeh@mail.ntust.edu.tw*

Bin-Chen Benson Hsiung
Department of Civil Engineering, National Chung Hsing University, Taiwan (R.O.C.)

ABSTRACT: Accurate prediction of wall deflections and ground settlements in deep excavations is critical for safety and performance in urban geotechnical engineering. However, conventional parameter calibration methods often rely on trial-and-error or empirical correlations, which are time-consuming and may not reflect true soil behavior. This study proposes an automated inverse analysis framework that integrates a multi-objective particle swarm optimization (MOPSO) with the hardening soil small-strain model (HS-small model) in PLAXIS 2D. A composite objective function is developed to capture three aspects of deformation mismatch: peak magnitude, location deviation, and overall shape, with higher penalties for underestimation to reflect design conservatism. The framework is validated using a real-world deep excavation case in Taiwan. Results are presented in the form of Pareto fronts, offering engineers a range of optimal solutions for balancing ground settlement and wall deflection performance. Comparative evaluation shows that the optimized parameters result in an agreement with field measurements. The proposed methodology demonstrates the potential of metaheuristic optimization to enhance reliability and efficiency in deep excavation modeling.

KEYWORDS: Deep excavation, HS-small model, PLAXIS 2D, MOPSO, inverse analysis

1 INTRODUCTION

Deep excavations can lead to significant ground deformations that may impact the structural integrity of nearby buildings and infrastructure. Accurate prediction of wall deflections and ground settlements in deep excavations is essential for effective risk management and optimizing design processes. Research utilizing finite element method software like PLAXIS, which incorporates advanced constitutive models for simulating deep excavations, has led to the development of a method for identifying soil parameters. Inverse analysis enables back-calculation of model parameters by minimizing the discrepancy between numerical predictions and field-monitored responses. Applied scripting for inverse analysis and stochastic simulations has recently gained popularity in geotechnical engineering (Aktaş Engin and Çokça, 2021; Eiesland, 2022).

Aktaş Engin and Çokça (2021) showed that metaheuristic algorithms could significantly enhance the robustness of inverse modeling in PLAXIS-based excavation simulations. Inverse analysis faces challenges because it is computationally intensive and often sensitive to initial parameter assumptions. The accuracy of results depends heavily on the quality of monitoring data and the structure of the objective function. Moreover, without a systematic search strategy, inverse procedures may converge to local optima or require excessive computational time. These limitations underscore the need for more intelligent, automated approaches to calibration.

Among various soil constitutive models, the hardening soil model with small-strain (HS-small) is particularly effective in capturing realistic deformation predictions, because it can capture the degradation of soil stiffness under small-strain conditions (Benz et al., 2009; Li et al., 2023). However, identifying HS-small model parameters remains a challenge. A typical parameter calibration way depends on empirical correlations and manual adjustments supported by visualizations. This process can be time-consuming and heavily reliant on the engineer's experience, which may limit objectivity (Ou, 2015; Teng, 2014). Additionally, laboratory testing alone often fails to accurately capture site-specific soil responses under complex loading conditions (Surarak et al., 2012). These reasons, as well as soil anisotropy and field variability (Teng et al., 2014), make it challenging to calibrate the constitutive model parameters. Especially, two key factors significantly affect predicted deformation patterns: the small-strain shear modulus G_0^{ref} and the shear strain parameter $\gamma_{0.7}$.

To address these challenges, metaheuristic optimization techniques have emerged as a systematic approach for solving inverse problems in geotechnical engineering (Coello Coello, 1999; Zhao et al., 2015) and offer potential to calibrate model parameters automatically by minimizing discrepancies between predicted and measured field data (Zhao et al., 2024).

This study aims to develop a Python-based multi-objective particle swarm optimization (MOPSO) framework to automate the calibration of key HS-small model parameters, the small-strain shear modulus G_0^{ref} and the shear strain parameter $\gamma_{0.7}$. The proposed optimization framework on real-world deep excavation projects, namely the Taipei National Enterprise Center (TNEC), is applied and validated to demonstrate the effectiveness of metaheuristic calibration methods. A novel and robust error assessment metric that enhances the accuracy and reliability of numerical excavation predictions is introduced. The performance of optimization results on wall deflection and ground settlement behaviors is demonstrated.

2 OPTIMIZATION AND AUTOMATION FRAMEWORK

This study presents an automated parameter calibration framework that integrates a finite element model built in PLAXIS 2D with a Python-implemented MOPSO algorithm. The framework aims to optimize two key small-strain stiffness parameters of the hardening soil model with small-strain stiffness: the initial shear modulus at very small strain (G_0^{ref}), and the reference shear strain ($\gamma_{0.7}$), which governs stiffness degradation. The goal is to improve agreement between numerical simulations and field measurements of wall deflections and ground settlements during deep excavations.

2.1 *Optimization framework*

The process begins with initializing the finite element model in PLAXIS 2D, where the excavation geometry, soil stratigraphy, constitutive models, and construction stages are defined. For

the optimization settings, Figure 1 shows the optimization framework, following a closed-loop structure. Each particle in the MOPSO algorithm represents a candidate set of HS-small model parameters across the critical soft clay layers. The algorithm iteratively updates these parameters, launches simulations via the PLAXIS remote scripting API, extracts deformation data, and evaluates fitness using MO error metrics.

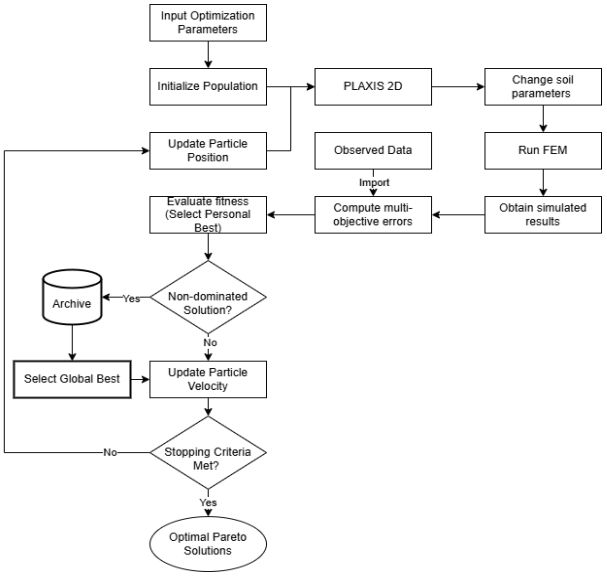

Figure 1. Optimization framework

2.2 *Objective function*

The simulation outputs, such as wall deflections and ground settlements, are extracted and compared to corresponding field data using objective error functions. A two-objective optimization problem is formulated:

- Objective f_1: Error in wall deflection
- Objective f_2: Error in ground settlement

Each objective is composed of three normalized components: peak error (E_{peak}), peak location deviation (E_{loc}), and shape error (E_{shape}). The total objective functions are computed using weighted sums:

$$f_1 = \alpha \,.\, E_{peak} + \beta \,.\, E_{loc} + \gamma \,.\, E_{shape} \tag{1}$$

$$f_2 = \alpha \,.\, E'_{peak} + \beta \,.\, E'_{loc} + \gamma \,.\, E'_{shape} \tag{2}$$

where:

f_1 is the objective function error of wall deflection

f_2 is the objective function error of ground settlement

$E_{peak}, E_{loc}, E_{shape}$ are the normalized errors of wall deflection

$E'_{peak}, E'_{loc}, E'_{shape}$ are the normalized errors of ground settlement

The weights are set as $\alpha = 0.5$, $\beta = 0.3$, and $\gamma = 0.2$, reflecting the dominant importance of peak magnitude in deformation matching.

2.3 *Decision variables and bounds*

Each particle in the optimization represents a decision vector $x = \{x_1, x_2, \ldots, x_n\}$, where each x_i corresponds to a specific HSsmall model parameter G_0^{ref} and $\gamma_{0.7}$ for a particular soft clay layer. These parameters are selected due to their significant influence on small-strain deformation behavior. The lower bound of G_0^{ref} is 15, and the upper bound is calculated using Equations (3) to (6).

$$\frac{G_0}{G_{ur}} \leq 20 \tag{3}$$

$$G_{ur} = \frac{E_{ur}^{ref}}{2(1+v)} \tag{4}$$

$$\text{Max } G_0^{ref} = 20 \times \frac{E_{ur}^{ref}}{2(1+V_{ur})} \tag{5}$$

$$G_0^{ref} = x_i \cdot \left(\frac{(2.973-e)^2}{1+e}\right) \cdot 1000 \text{ MPa} \tag{6}$$

While the lower bound and upper bound of the $\gamma_{0.7}$ are shown below.

$$1 \times 10^{-5} < x_i < 1 \times 10^{-4} \tag{7}$$

These bounds ensure realistic strain-dependent softening behavior in the HS-small model and allow the optimization to search efficiently within a relevant domain.

2.4 *MOPSO optimization procedure*

The core of the calibration process is driven by a customized multi-objective particle swarm optimization algorithm designed to efficiently explore the multi-dimensional solution space. Each particle in the swarm represents a candidate solution, comprising a set of pre-factors (x_i) that scale the small-strain shear modulus (G_0^{ref}) and reference shear strain ($\gamma_{0.7}$) for each relevant soil layer.

The particles are initialized within geotechnically realistic bounds and evolved over iterations using the standard PSO velocity and position update equations:

$$v_i^{t+1} = \chi[w{v_i}^t + c_1 r_1\left(P_{best,i} - {x_i}^t\right) + c_2 r_2(G_{best} - {x_i}^t)] \tag{8}$$

$${x_i}^{t+1} = {x_i}^t + v_i^{t+1} \tag{9}$$

where w is the inertia weight, c_1 and c_2 are cognitive and social acceleration coefficients; r_1 and r_2 are randomly generated numbers in the range [0, 1]; $P_{best,i}$ is the particle's personal best position; G_{best} is the global best leader selected from the archive. In MOPSO, elitism is implemented by maintaining an external archive of non-dominated (elite) solutions. By choosing G_{best} from the elite archive and updating P_{best} only if a particle finds a better non-dominated solution, elitism helps preserve non-dominated solutions and improves convergence toward the Pareto front.

To ensure physical feasibility and compatibility with the PLAXIS model, each updated position is bounded within predefined parameter limits using a clamping strategy. This is implemented in the optimization code using a vectorized bounding function that limits the position to lie between the lower and upper bounds.

This velocity–position update mechanism enables each particle to explore the parameter space dynamically while leveraging both individual and global knowledge, ensuring convergence toward diverse, high-quality solutions on the Pareto front.

2.5 *Pareto front evaluation and solution selection*

The final output of the optimization is a Pareto front consisting of non-dominated solutions representing trade-offs between wall deflection and ground settlement accuracy. The quality of this front is assessed using the hypervolume metric, which quantifies the area in objective space dominated by the front to a predefined reference point. Monte Carlo sampling with one million points is used for hypervolume estimation, with higher values indicating better convergence and diversity.

This study also reports the associated standard error, which quantifies the statistical uncertainty of the result due to random sampling. It is calculated based on the empirical proportion of samples falling within the dominated region of the objective space, using Equation (10):

$$Standard\ error = \sqrt{p(1-p)/N} \tag{10}$$

where p is the proportion of dominated samples and N is the total number of Monte Carlo samples. A smaller standard error indicates a more precise and reliable estimate of the hypervolume.

2.6 *Solution visualization*

Once the representative solutions are selected from the Pareto front, they are re-simulated in PLAXIS to verify their performance against field observations. The resulting deflection profiles—both for wall deflection and ground settlement—are directly compared to the corresponding measured data to assess the accuracy of the calibration. Each error component, including peak deviation, location offset, and profile shape, is individually evaluated to confirm improvement over prior estimates or baseline assumptions.

3 TNEC CASE STUDY

This study utilizes the PLAXIS 2D finite element platform to simulate deep excavation behavior. The TNEC case is used to validate the proposed optimization-based calibration framework. The structure properties, including bracing system, retaining wall, groundwater and dewatering system, excavation and construction sequence, and overall deformation patterns at various excavation stages, are based on Ou et al. (2000).

This case features alternating layers of silty clay (CL) and silty sand (SM), with six main layers called Sungshan I through VI. A key aspect is the 25-meter-thick silty clay layer (Sungshan IV), which affects excavation-induced soil deformation due to its compressibility and low shear strength. This layer has an over-consolidation ratio (OCR) of 1.03 to 1.72, a liquid limit of 29% to 39%, and an average plasticity index of about 17%. Its undrained shear strength to effective overburden stress ratio is 0.32 to 0.36 from unconsolidated undrained and field vane shear tests (Ou et al., 2000; Teng, 2014).

3.1 *Optimization settings for the MOPSO*

The selected swarm settings and control parameters used to calibrate HS-small parameters are summarized in Table 1, where they are adopted based on accepted recommendations for multi-objective swarm algorithms and tuned through preliminary trials (Lin & Xu, 2015; Moravec & Rudolf, 2017).

Table 1. Parameter configuration for the MOPSO

Parameter	Value	Description
Swarm size	20	Number of particles
Maximum iterations	50	Upper limit of optimization generations
Cognitive coefficient (c_1)	2	Personal memory weight
Social coefficient (c_2)	2	Swarm memory weight
Inertia weight	0.9 → 0.4	Linearly decaying inertia across iterations

3.2 *Soil parameters in PLAXIS2D*

The HS-small model is selected for clay under undrained conditions (Undrained A), while the hardening soil (HS) model is adopted for sand under drained conditions. Table 2 presents the physical and mechanical properties of the soils, whereas Table 3 summarizes the initial input parameters of the decision variables for the soil models. The decision variables include G_0^{ref} and $\gamma_{0.7}$ for each clay layer, resulting in a total of 22 decision variables.

The search space—defined by the upper and lower bounds for each variable—is determined based on empirical correlations and engineering judgment. The pre-factors are calculated according to the methodology outlined in Section 2.3.

Table 2. Physical and mechanical properties of soils

Layers' name (depth~depth m)	E_{50}^{ref} kPa	E_{oed}^{ref} kPa	E_{ur}^{ref} kPa	ϕ °	c kPa	γ_{unsat} kN/m^3
CL11 (0~2)	7738	5416	23214	29	0	18.25
CL12 (2~4)	7667	5367	23000	30	0	18.25
CL13 (4~5.6)	7557	5290	22670	30	0	18.25
SM1 (5.6~8)	9707	9707	29121	31	0	18.93
CL21 (8~12)	7844	5491	23531	29	0	18.15
CL22 (12~16)	7998	5598	23993	29	0	18.15
CL23 (16~20)	8335	5835	25006	29	0	18.15
CL24 (20~24)	8383	5868	25149	29	0	18.15
CL25 (24~27)	8577	6004	25730	29	0	18.15
CL26 (27~30)	8784	6149	26353	29	0	18.15
C27 (30~33)	9007	6305	27022	29	0	18.15
SM2 (33~35)	13671	13671	41014	31	0	19.62
CL31(35~37.5)	9247	6473	27742	30	0	19.13
SM3 (37.5~41.5)	18368	18368	55105	32	0	19.62
SM4 (41.5~59)	22148	22148	66443	32	0	19.62

Table 3. Initial input parameters for soils

Name	E_{ur}^{ref}	Max. G_0^{ref}	Min. G_0^{ref}	Max. Pre-factor	Max. Pre-factor, Max. and Min. $\gamma_{0.7}$
CL11	23214	138180	46945	44.15	Min. Pre-factor =15
CL12	23000	133723	44268	45.31	
CL13	22670	129544	42358	45.87	
CL21	23531	121924	32439	56.38	
CL22	23993	125618	33424	56.38	Max. $\gamma_{0.7}$ = 1E-04
CL23	25006	133723	35475	56.54	
CL24	25149	138180	38204	54.25	
CL25	25730	142945	39349	54.49	Min. $\gamma_{0.7}$ = 1E-05
CL26	26353	148050	40527	54.80	
CL27	27022	153533	41739	55.18	
CL31	27742	159438	42985	55.64	

4 RESULTS AND DISCUSSIONS

This optimization approach simultaneously minimized the errors between simulated and measured wall deflections and ground surface settlements. Due to stagnation, this optimization stopped at the 35th iteration, with a total time elapsed of 91,433 sec, and the average time of each iteration being 2,500 sec.

4.1 *Selection of the optimal solution set*

Figure 2 presents the Pareto front, where the x-axis represents the wall deflection error and the y-axis represents the ground settlement error. The number of Pareto solutions is 14. Three representative solutions from the Pareto front are selected to reflect different optimization priorities:

- Solution 12 – Minimum wall deflection error: This solution, located at the upper-left edge of the Pareto front, prioritizes minimizing wall deflection error despite its large ground settlements. (See Figure 3)
- Solution 10 – Minimum ground settlement error: Positioned at the lower-right edge of the Pareto front, this solution minimizes ground settlement error and is suitable for cases where surface deformation control is critical. (See Figure 4)
- Solution 3 – Balanced Trade-Off Solution: The solution is based on the shortest Euclidean distance to the origin (0,0) in the normalized objective space. This solution compromises wall deflection and ground settlement, and is generally the most practical for general excavation projects. (See Figure 5)

4.2 *Hypervolume evaluation*

The hypervolume metric is calculated using a Monte Carlo simulation, as detailed in Section 2.5. A reference point of (0.0861, 0.1687) is set to define the objective space based on 5% of the maximum wall deflection and ground settlement

errors. Table 4 summarizes the hypervolume analysis, showing a low standard error of the estimate, 0.000003, which suggests good visual quality of the Pareto front, even though the hypervolume value is lower than expected for more evenly distributed objective spaces.

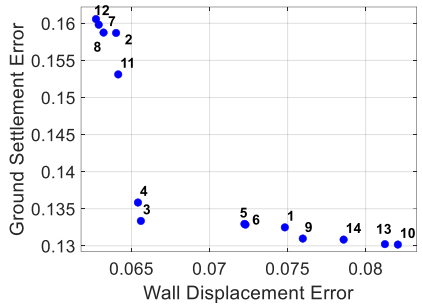

Figure 2. Pareto front solutions

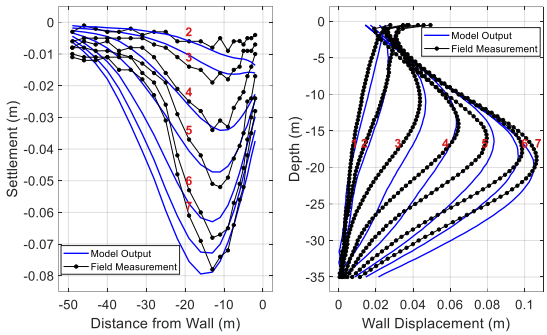

Figure 3. Solution 12 – minimize wall deflection error.

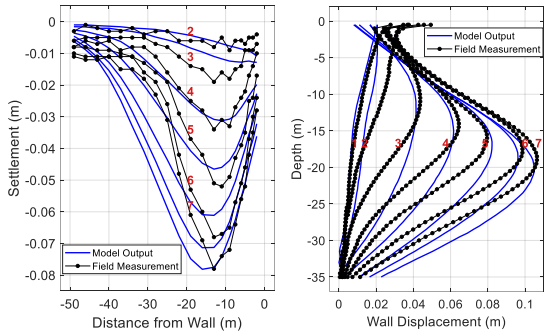

Figure 4. Solution 10 – minimize ground settlement error.

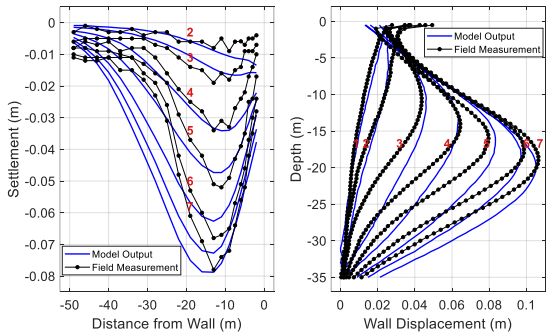

Figure 5. Solution 3 – balanced error.

Table 4. Hypervolume evaluation summary for TNEC Case

Metric	Value
Monte Carlo samples	1,000,000
Hypervolume estimate	0.000794
Approximate standard error	0.000003
Normalized hypervolume estimate	0.0546 ≈ 5.5 %

5 CONCLUSIONS

This study developed and validated a robust optimization framework that combines multi-objective calibration with finite element modeling to enhance the prediction of deep excavation behavior. Using the MOPSO and small-strain stiffness parameters are calibrated based on observed wall deflections and ground settlements. The key findings are summarized as follows:

- Integrating MOPSO with PLAXIS 2D enables accurate calibration of HS-small model parameters, reducing discrepancies between numerical results and field data.
- The Pareto front solutions offer engineers various calibration solutions for different performance needs.
- The calibrated small-strain stiffness parameters can be utilized to create specific parameter ranges for different soil types, aiding in developing reference parameter libraries.

The proposed optimization framework effectively back-analyzes deep excavation behavior and shows promise for future applications. It can integrate additional objective functions, allow real-time calibration during construction, and adapt to advanced soil models.

6 ACKNOWLEDGEMENTS

This work is supported by the National Science and Technology Council (NSTC), Taiwan, R.O.C., under project numbers NSTC 113-2625-M-011-005 and 114-2221-E-011-011-MY2.

7 REFERENCES

Aktaş Engin, T., & Çokça, E. 2021. Automated inverse analysis of a deep excavation in Ankara clay using finite element analysis. *Arabian Journal of Geosciences* 14(19), 1991.

Benz, T., Schwab, R., Vermeer, P., 2009. Small-strain stiffness in geotechnical analyses. *Bautechnik* 86, 16–27.

Coello Coello, C.A.. 1999. A Comprehensive Survey of Evolutionary-Based Multiobjective Optimization Techniques. *Knowledge and Information Systems* 1(3), 269-308.

Eiesland, O. 2022. Implementation of random finite element method in Plaxis Using API / Python scripting, Master's Thesis, Norwegian University of Science and Technology, Norway.

Li, Y.-X., Abdi, A. S., Teng, F., & Ou, C.-Y. 2023. Numerical Evaluation On The Application Of Small Strain Stiffness Model For Deep Excavations In Soft Clays. *Journal of GeoEngineering* 18(3), 103-116.

Lin, X., & Xu, Z. 2015. Swarm size and inertia weight selection of Particle Swarm Optimizer in system identification. *2015 4th International Conference on Computer Science and Network Technology (ICCSNT)*.

Moravec, P., & Rudolf, P. 2017. Application of a particle swarm optimization for shape optimization in hydraulic machinery. *EPJ Web of Conferences*.

Ou, C.-Y. 2015. Finite element analysis of deep excavation problems. *Journal of GeoEngineering* 11, 1-12.

Ou, C.-Y., Bor-Yuan, S., & I-Wen, W. 2000. Three-dimensional deformation behavior of the Taipei National Enterprise Center (TNEC) excavation case history. *Canadian Geotechnical Journal* 37(2), 438-448.

Teng F.-C., Ou C.-Y., & Hsieh P.-G. 2014. Measurements and Numerical Simulations of the Inherent Stiffness Anisotropy in Soft Taipei Clay, *Journal of Geotechnical and Geoenvironmental Engineering* 140(1), 237-250

Zhao, B. D., Zhang, L. L., Jeng, D. S., Wang, J. H., & Chen, J. J. 2015. Inverse Analysis of Deep Excavation Using Differential Evolution Algorithm. *International Journal for Numerical and Analytical Methods in Geomechanics* 39(2), 115-134.

Zhao, C., Chen, L., Ni, P., Xia, W., & Wang, B. 2024. A modified back analysis method for deep excavation with multi-objective optimization procedure. *Journal of Rock Mechanics and Geotechnical Engineering* 16(4), 1373-1387.